ANL/CP--71551 12

DE91 018571

Transport Properties and Oxidation in Chromium and Fe-Cr Alloys Exposed to Oxygen at High Temperatures*

J.-H. Park and K. Natesan

Materials and Components Technology Division
Argonne National Laboratory, Argonne, Illinois 60439

SEP 2 0 1991

March 1991

The submitted manuscript has been authored by a contractor of the U. S. Government under contract No. W-31-109-ENG-38. Accordingly, the U. S. Government retains a nonexclusive, royalty-free license to publish or reproduce the published form of this contribution, or allow others to do so, for U. S. Government purposes.

Manuscript to be submitted for the International Conference on Heat Resistant Alloys at High-Temperatures, September 22-26, Lake Geneva, WI.

*Work supported by the U. S. Department of Energy, Advanced Research and Technology Development, Fossil Energy Materials Program, under Contract W-31-109-Eng-38.

DISCLAIMER

This report was prepared as an account of work sponsored by an agency of the United States Government. Neither the United States Government nor any agency thereof, nor any of their employees, makes any warranty, express or implied, or assumes any legal liability or responsibility for the accuracy, completeness, or usefulness of any information, apparatus, product, or process disclosed, or represents that its use would not infringe privately owned rights. Reference herein to any specific commercial product, process, or service by trade name, trademark, manufacturer, or otherwise does not necessarily constitute or imply its endorsement, recommendation, or favoring by the United States Government or any agency thereof. The views and opinions of authors expressed herein do not necessarily state or reflect those of the United States Government or any agency thereof.

MASTER

DISTRIBUTION OF THIS DOCUMENT IS UNLIMITED

Transport Properties and Oxidation in Chromium and Fe-Cr Alloys Exposed to Oxygen at High Temperatures*

J.-H. Park and K. Natesan

Materials and Components Technology Division
Argonne National Laboratory, Argonne, Illinois 60439

Abstract

Alloy samples of Fe-25Cr, Fe-25Cr-0.3 and 1Y, and Fe-25Cr-1Ce were subjected to oxidation tests in a microbalance at temperatures between 700 and 1000°C and at oxygen partial pressures in a range of 1 to 10^{-20} atm for time periods of 19 to 160 h. Integrity of the scales was also evaluated by quenching from the oxidation temperature to room temperature in ~20 minutes. During quenching, the 24-h oxidized samples of Fe-25Cr showed total spallation of oxide layers from the alloy substrate. However, the Y- and Ce-containing alloys did not show scale spallation during thermal quenching. To determine total spallation behavior in Fe-25Cr, the oxidation and quenching tests were repeated twice with the same samples. To learn why the scale in the second and third oxidation/quenching runs did not spall as in the first run, we focused on alloy grain growth behavior during oxidation. Cation mixing properties obtained by electrical conductivity measurements on oxidized specimens were compared with the oxygen diffusivity in the corrosion product formed on the Fe-25Cr alloy.

Introduction

Corrosion resistance of structural alloys in high-temperature environments is achieved by the formation of a continuous chromium oxide (Cr_2O_3) scale. [1] This scale can be treated principally as a rate-determining solid-state diffusion barrier between the environment and the alloy substrates. High temperature oxidation studies have two fundamental aspects; elucidating the transport mechanisms to reduce oxidation kinetics and improving adhesion of the scale to the base alloy substrate. [2] When alloys contain so called “reactive elements” or “oxygen active elements”, i.e, Y, La, and Ce, etc., the growth rate of the oxide layer is reduced and

---

*Work supported by the U. S. Department of Energy, Advanced Research and Technology Development, Fossil Energy Materials Program, under Contract W-31-109-Eng-38.

adhesion of the oxide layer to the base alloy is enhanced. [3]

The objective of the present work is to observe the overall schemes for the oxidation behavior for the chromia forming alloys of Fe-25Cr with and without additions of reactive elements (such as Ce, and Y).

Experimental Procedure

Thermogravimetric analysis (TGA) of oxidation of Fe-25Cr

Oxidation studies were performed on samples of Fe-25Cr, Fe-25Cr-0.3Y with a CAHN electrobalance. The samples were suspended by a platinum wire, and a reaction gas was admitted from the bottom of the reaction chamber. The samples were heated in the reaction gas to the desired temperature, and changes in sample weight were monitored continuously. Oxidation temperature range was 700 - 1000°C and oxygen partial pressures were controlled by flowing different gases, namely, oxygen, air, 1 vol.%CO-CO_2, and 18 vol.%CO-CO_2 . After cooling the oxidized samples were examined with a SEM (scanning electron microscope): Both the surface and the the cross section of cold-mounted samples were evaluated.

Another set of samples of Fe-25Cr (as received and enlarged grain size), Fe-25Cr-1Y, and Fe-25Cr-1Ce was oxidized at 1000°C in an oxygen-nitrogen gas mixture with a $pO_2 = 10^{-4}$ atm.

Electrical resistivity of oxidized foils.

Electrical resistivity of the oxidized samples of Fe-25Cr and Fe-25Cr-1Ce was measured by a standard four-probe method at a fixed DC current from a Keithley Calibrator/Source Model 263 over a range of 10-100 μA.

Results and Discussion

Oxidation of Fe-25Cr and Fe-25Cr-0.3Y

Figure 1 shows calculated equilibrium oxygen partial pressures for several gas mixtures and metal/metal oxides as a function of temperature. Figure 2 shows the TGA test data for Fe–25Cr alloy oxidized in air and Figure 3 shows weight-change versus time for oxidation of Fe-25Cr and Fe-25Cr-0.3Y alloysin the gas mixtures of 1 vol.%CO-CO_2 and 18 vol.%CO-CO_2 at 1000°C. The weight change of the Fe-25Cr alloy exposed to 1 vol.%CO-CO_2 shows much higher rate than that of others. This behavior could be explained by the composition of the growing scale. i.e., the sample surface was completely covered with an $Fe_{3-\delta}O_4$ at outer surface and an $Fe_{1-\delta}O$ inner scale. [4] However, in the case of 18 vol.%CO-CO_2gas mixture, no iron oxide or large grain scale was observed on the sample surface, because the pO_2 value was not sufficient to form iron oxides. At other temperatures and oxygen partial pressures, tests did not show any significant difference in oxidation rates were even though a small amount of iron was observed in the oxide scales based on the TGA data and visual observation of the cross sections of the oxidized scales. At high oxygen partial pressures, the formation of hematite [$Fe_2O_{3-\delta}$] is expected. Hematite has the same crystal structure as chromium oxide, i.e., corundum structure, which would be expected to have diffusion properties similar to those of chromium oxide.

Oxide scales on always with small amount of yttrium contained no iron oxide over the wide range of temperature and oxygen partial pressure of the present investigation. The absence of iron oxide may be explained by the predominance of anion transport. [1,5] However, the values of the parabolic rate constant were similar for alloys with and without reactive elements, and the oxidation process seemed to be controlled by ionization of chromium at the scale/alloy interface. At 700°C and low oxygen partial pressures, calculated scale thickness from weight-change data by TGA exceeds the measured scale thickness by SEM, which indicates that internal oxidation or solubility of some species within the metal occurs.

Oxidation of Fe-25Cr, Fe-25Cr-1Ce, and Fe-25Cr-1Y at 1000°C

After 19 h oxidation and thermal quench of a Fe-25Cr specimen, the oxide scale separated from the substrate. At high magnifications, 1-μm edge cracks were apparent in the 15 - 20 μm scale near the scale/alloy interface. In addition, scale bending due to plasticity of the scale at elevated temperatures and scale spallation due to thermal expansion mismatch between the scale and substrate alloy were observed.[6] SEM and EDS analyses of the fracture surfaces of the spalled oxide scales showed that the scales were pore-free pure chromia. The presence of grinding/scratch marks remaining on the interface (i.e., scale/alloy interface of the spalled oxide) indicates that outward diffusion of cations through the oxide scale was dominant, similar to marker experiments. [7,8] Beneath the spalled scale the alloy side of the scale/metal interface showed a number of small crystals. EDS analysis indicated these crystals were Cr_2O_3. Crystal growth near the interface can be explained by;

(1) vapor phase transport of chromium at the reduced oxygen partial pressure at the alloy/scale interface,

(2) separation of alloy/scale interface at an earlier stage of the oxidation,

(3) gap between alloy substrate and scale could be wider than the crystal dimension, which is in this case about 1 μm, and

(4) the possibility of inward oxygen diffusion through the scale.

Grain-boundaries in the alloy substrate exhibited very fine grooving at the alloy surface, to a depth similar to the oxide grain size. This indicates good adhesion between scale and alloy substrate in the early stage of oxidation. No scale spallation was observed in the reoxidized sample after thermal quenching treatment.

For longer oxidation times, weight change versus time curves showed an abrupt increase in weight gain. A typical plot is shown in Fig. 2 for a Fe-25Cr specimenat 1000°C in high oxygen partial pressure. Initially, a chromia scale formed and after ~100 h, the scale became covered with fast–growing iron oxide.

From this sudden increase in weight gain, outward transport of iron and subsequent oxidation are dominant features in long–term oxidation.[9] Typical chemical compositions of the scale layer after ~200 h exposure are listed in Table 1.

Table 1. Chemical compositions from EDS analysis of scale on Fe-25Cr.

Scale location	Cation composition
outer scale	Fe
thin scale (outer)	3Fe-97Cr
outer middle scale	50Fe-50Cr
inner middle scale	51Fe-49Cr
thin scale (inner)	1Fe-99C

Visual observations were made of the scales and alloy substrates before and after oxidation experiment. Enlarged alloy grains were observed in Fe-25Cr alloys after exposure. Since substantial grain growth in alloy substrate was observed, further studies focused on grain growth during oxidation of alloys with and without Y addition. [9]

According to literature, solid solubility of yttrium in chromium is 0.71 atomic percent and that of chromium in yttrium is 0.70 atomic percent. However, the difference in the respective atomic radii of Cr and Y as well as parametric data, [10] suggests that the solid solubility of Y in Cr is < 0.005 atomic percent. In the Fe-Y phase diagram, a stable compound Y_2Fe_{17} with an hexagonal structure has been identified. In previous studies on Fe-25Cr-0.87Y alloy, $Y_2(Fe, Cr)_{17}$ was identified in alloy grain-boundary. [11]

Samples of Fe-25Cr and the Y–containing alloy were oxidized, cold mounted for SEM, and etched in slightly acidic solution to dissolve the alloy around the scale to examine the scale microstructure. The cross sections of the Fe-25Cr specimens showed large differences in grain size after oxidation at temperatures between 700 - 1000°C. However, in Fe-25Cr-1Y no grain-growth was observed (Fig. 4). At temperatures below 800°C, no significant grain growth occured in either of the alloys.

Oxidation of Fe-25Cr after vacuum anneal at 1000°C for 24 h

In order to investigate the scale spallation in the Fe-25Cr alloy and the causes for the grain-growth during oxidation, alloy samples of Fe-25Cr were annealed in vacuo at 1000°C for 24 h 40 min and then were oxidized for 20 h. Weight change versus time behavior was compared with the oxidation behavior of an as–received sample (1st run) and a spalled sample (2nd run). The oxidation behavior of the annealed sample, which had an enlarged grain size was, similiar to that the spalled sample (2nd run). No spallation was observed after the thermal quenching of the annealed sample.

Electrical resistivity of oxidized foils

Figure 5 shows the log ohmic resistance versus reciprocal temperature for the oxide Fe-25Cr and Fe-25Cr-1Ce alloys. The ohmic resistance of the oxide scales formed on the Ce-containing alloy was higher than that of the scale on the Fe-25Cr alloy. These results can be analyzed by the defect incorporation scheme described below. In the high-pO_2 region, the most stable valence state of cerium is +4. When cerium is incorporated into the cation sublattices at either Cr (+3) or Fe (+3) site,

$$CeO_2 = Ce^{\bullet}_{Cr\ (or\ Fe)} + 1/2\ O_2\ (g) + 3/2\ O^{x}_{o} + e'. \tag{1}$$

Similarly, when we consider the cation interstitial as a point defect, incorporation of the cerium ion may be written as

$$CeO_2 = Ce^{\bullet}_{i} + 1/2\ O_2\ (g) + 3/2\ O^{x}_{o} + e'. \tag{2}$$

In either case, electrons are produced as a charge-compensating defect. The electron holes are annihilated by recombination with electrons, i.e.,

$$nil = e' + h^{\bullet}. \tag{3}$$

Consquently, the ohmic resistance increases, i.e., electrical conductivity decreases. Our studies indicate that Cr_2O_3 is predominantly a p-type semiconductor, [12] as is the oxide developed on Fe-25Cr.

In order to observe the cation mixing kinetics for Fe/Cr in the alloy oxide, the ohmic value was monitored as a function of time to obtain diffusion information. In the diffusion analysis, a thin-plate model was introduced with the condition of no oxygen chemical potential gradient accross the sample. Results for the apparent and bulk diffusivity are plotted in Fig. 6. The apparent diffusivity is based on the overall thickness of the specimen, whereas the oxide grain size was considered in calculating the bulk diffusivity. Oxygen diffusion data, obtained from literature, are also plotted.[13,14] The data indicate that at high temperatures, anion inward diffusion becomes a possibility during the oxidation of Fe-25Cr when iron becomes mixed in the scale. However, at lower temperatures, cation outward diffusion is expected, based on the data in Fig. 6.

Conclusions

1) The major role of reactive elements in oxidation is to suppress iron diffusion through the scale.

2) Reactive elements also inhibit grain growth in the alloy. Consquently, no spallation of thermally grown scale was observed even under thermal quenching conditions

3) In alloys without reactive elements scale spallation was minimized by a large alloy grain size. However, outward diffusion of iron occurred similar to that in alloy with normal grain size.

4) Alloy grain growth in decreasing order is as follows:
Fe-25Cr >> Fe-25Cr-1Ce > Fe-25Cr-1Y.

Acknowledgments

This work was supported by the U.S. Department of Energy, Advanced Research and Technology Development Fossil Energy Materials Program, under Contract W-31-109-Eng-38. D. L. Rink assisted with the experimental aspects of the program.

References

1. P. Kofstad, High Temperature Corrosion (Elsevier Applied Science, England, Essex, 1988); Nonstoichiometry, Diffusion and Electrical Conductivity in Binary Metal Oxides (Wiley Interscience, New York, 1972)

2. A. Rahmel, G. C. Wood, P. Kofstad, and D. L. Douglass, International Workshop on "Critical Issues Concerning the Mechanisms of High-Temperature Corrosion", Oxid. Metals, 23 (5/6) 251 (1985)

3. L. B. Pfeil, "Improvements in Heat Resistant Alloys," Brit. Pat. No. 459848 (1937)

4. R. Dieckmann, Diffusion of Cations and of Point Defects in Magnetite, *Proc. Symp. Metall. Soc. AIME and MSD-ASM Atomic Transport Activity,* TMS-AIME Fall Meeting, Orlando, FL, Oct. 6-7 (1986): p. 7

4. J.-H. Park, K. Natesan, and D. L. Rink, Sulfur and Oxygen Transport Properties of Thermally Grown Cr_2O_3 Film, to be published in High Temperature Science

5. W. E. King and J.-H. Park, Coll. De Phys. 51, C1-551-556 (1990)

6. A. G. Evans and R. M. Cannon, Stresses in Oxide Film and Relationship with Cracking and Spalling, *Proc. Symp. Metall. Soc. AIME and MSD-*

ASM Atomic Transport Activity, TMS-AIME Fall Meeting, Orlando, FL, Oct. 6-7 (1986): p. 135

7. C. S. Giggings and F. S. Pettit, Trans. Metall. Soc. AIME, 245 2495 (1969)

8. P. Kofstad and A. Z. Hed, Werkst. Korros., 21 894 (1970)

9. J.-H. Park and K. Natesan, **manuscripts for** ANL FE/91-?

10. M. Hansen, Constitution of Binary Alloys (McGraw-Hill Book Co., New York, 1958)

11. W. E. King, N. L Peterson and J. F. Reddy, J. Physique, 46, C4-423 (1985)

12. J.-H. Park and K. Natesan, Electronic Transport in Thermally Grown Cr_2O_3, Oxi. Metals, 33(1/2) 31 (1990)

13. M. J. Graham, J. I. Eldridge, D. F. Mitchell and R. J. Hussey, *Mater. Sci. Forum* 43, 207 (1989)

14. J.-H. Park and K. Natesan, Transport Properties of Chromium and Fe-Cr Alloys Exposed to Oxygen/Sulfur Environments, Fourth Berkeley Conf. on Corrosion-Erosion-Wear of Materials at Elevated Temperatures, January 31 -February 2, 1990, Berkeley, California, to be published by NACE

FIGURES

Figure 1.	Log pO_2 versus inverse temperature for various gas mixtures and metal/oxide equilibria.
Figure 2.	Weight change versus time during oxidation of Fe-25Cr and Fe-25Cr-0.3Y alloys at low oxygen partial pressures.
Figure 3.	Weight change versus time during oxidation of Fe-25Cr at high oxygen partial pressures.

Figure 4 Grain size of Fe-25Cr and Fe-25Cr-1Y alloys after oxidation at temperatures between 700 and 1000°C for time period of 90 to 135 h.

Figure 5. Log (R, ohmic resistance) versus inverse temperature for oxidized foil samples of Fe-25Cr and Fe-25Cr-1Ce.

Figure 6. Temperature dependence of cation and oxygen diffusion in thermally growing scales on chromium and Fe-25Cr alloys.

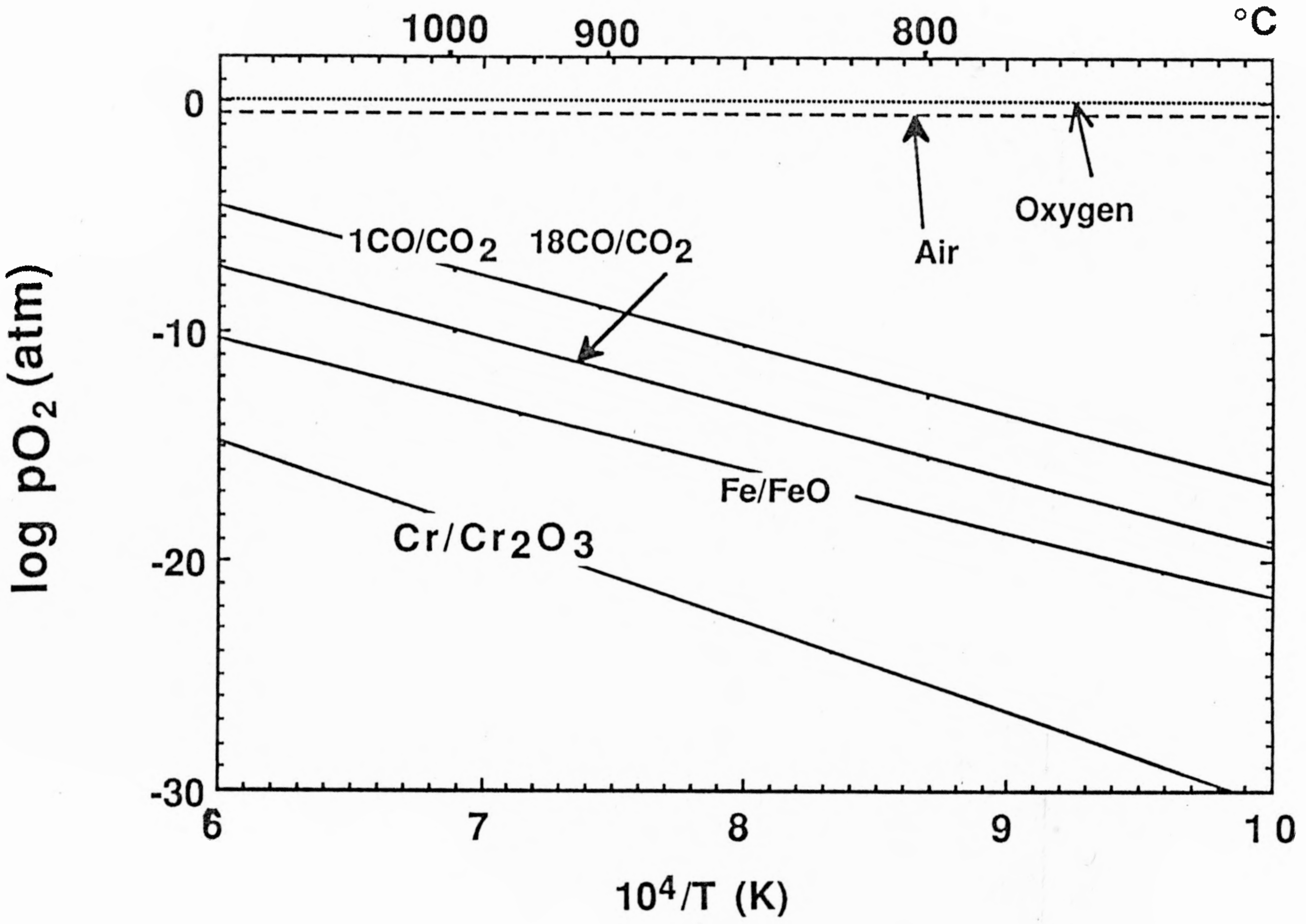
1000
900
800
°C
0
-10
-20
-30
6
7
8
9
10
log pO_2 (atm)
10^4/T (K)
Oxygen
Air
$1CO/CO_2$
$18CO/CO_2$
Fe/FeO
Cr/Cr_2O_3

①

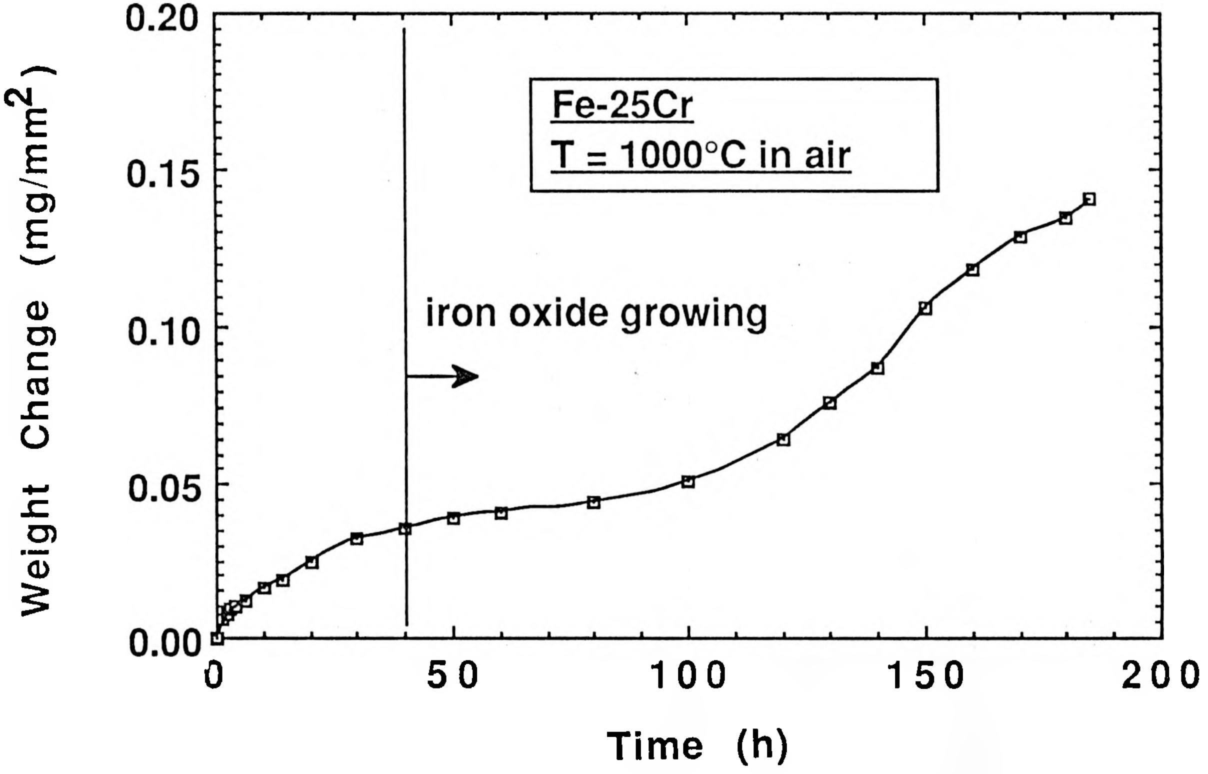
Fe-25Cr
T = 1000°C in air
iron oxide growing
Weight Change (mg/mm²)
Time (h)
0.00
0.05
0.10
0.15
0.20
0
50
100
150
200

(2)

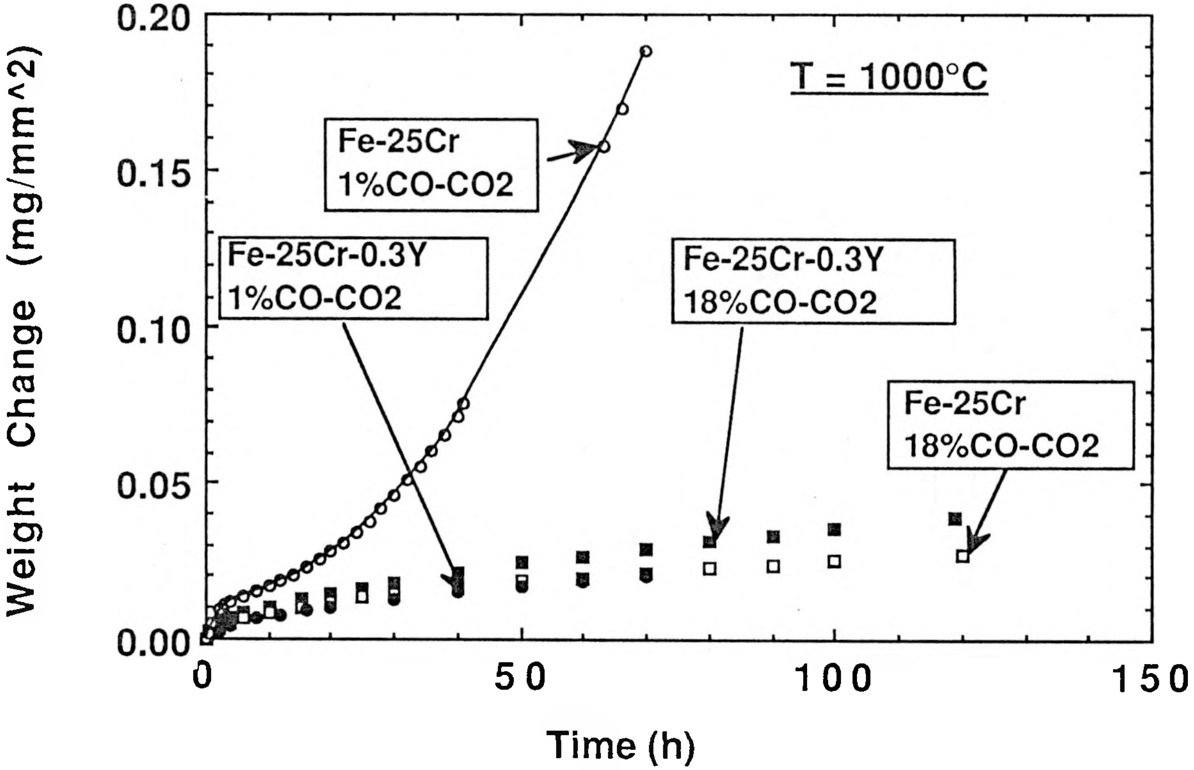
T = 1000°C
Fe-25Cr
1%CO-CO2
Fe-25Cr-0.3Y
1%CO-CO2
Fe-25Cr-0.3Y
18%CO-CO2
Fe-25Cr
18%CO-CO2
Weight Change (mg/mm^2)
0.20
0.15
0.10
0.05
0.00
0
50
100
150
Time (h)

③

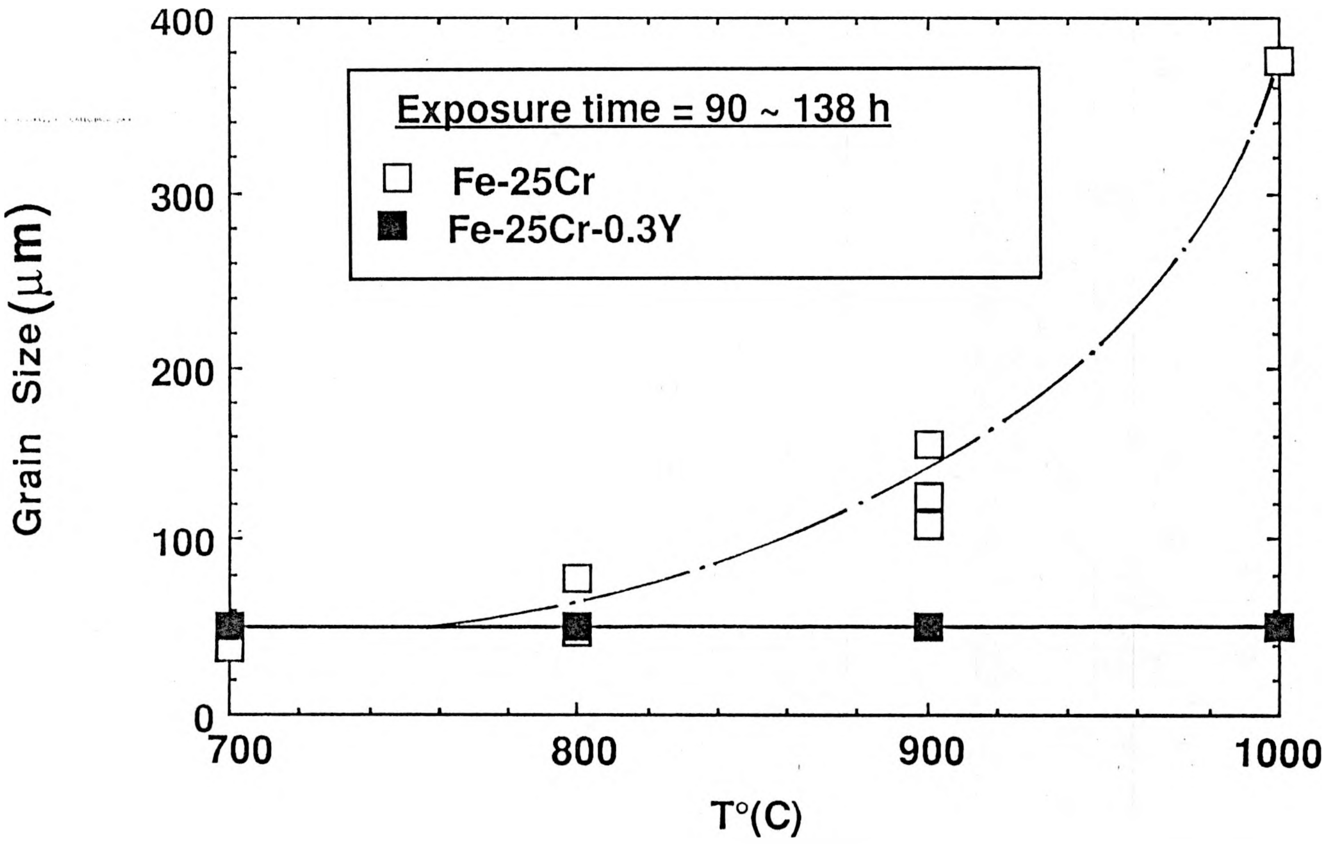
Exposure time = 90 ~ 138 h
□ Fe-25Cr
■ Fe-25Cr-0.3Y
Grain Size (μm)
400
300
200
100
0
700
800
900
1000
T°(C)

(4)

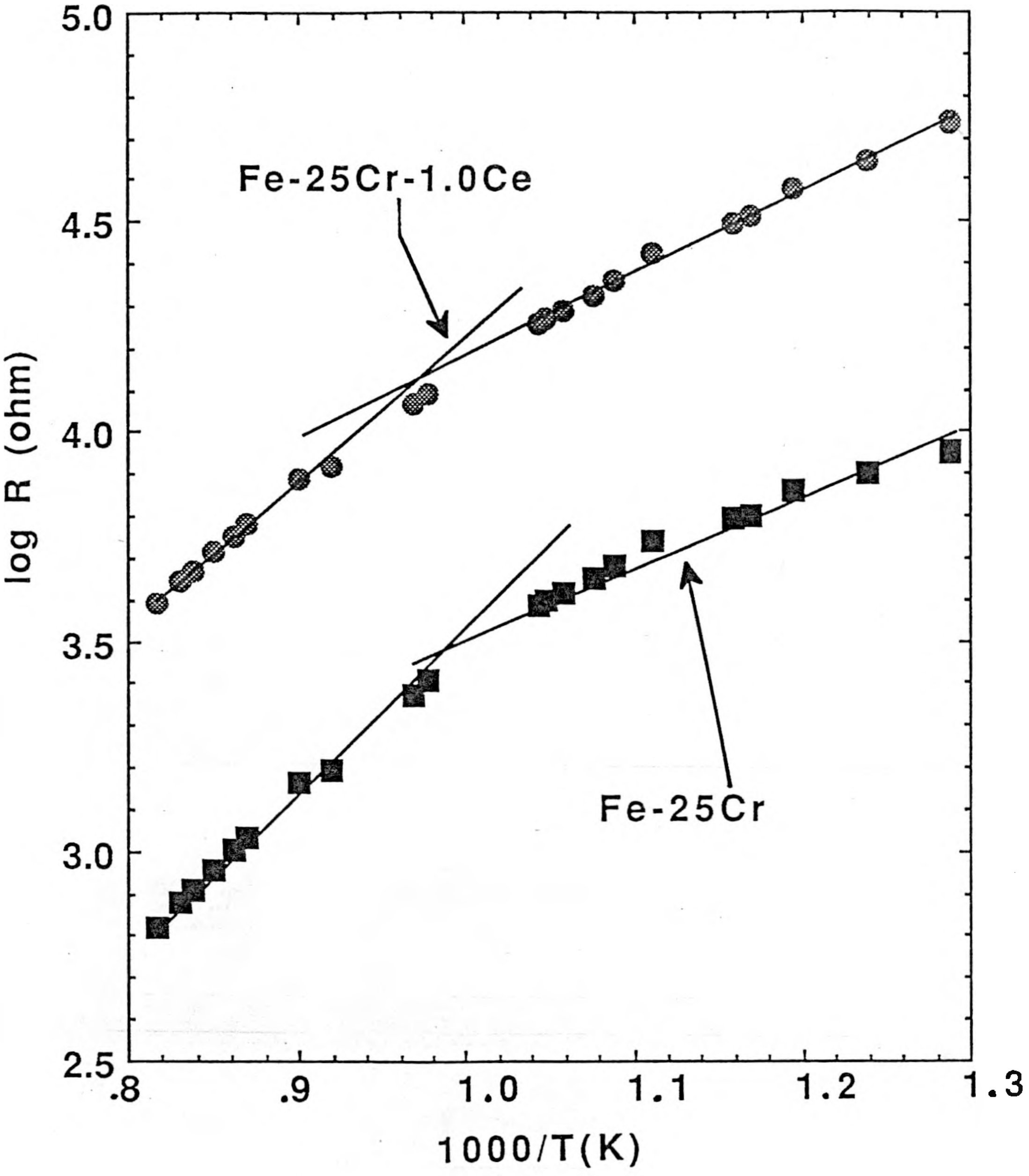
Fe-25Cr-1.0Ce
Fe-25Cr
log R (ohm)
5.0
4.5
4.0
3.5
3.0
2.5
.8
.9
1.0
1.1
1.2
1.3
1000/T(K)

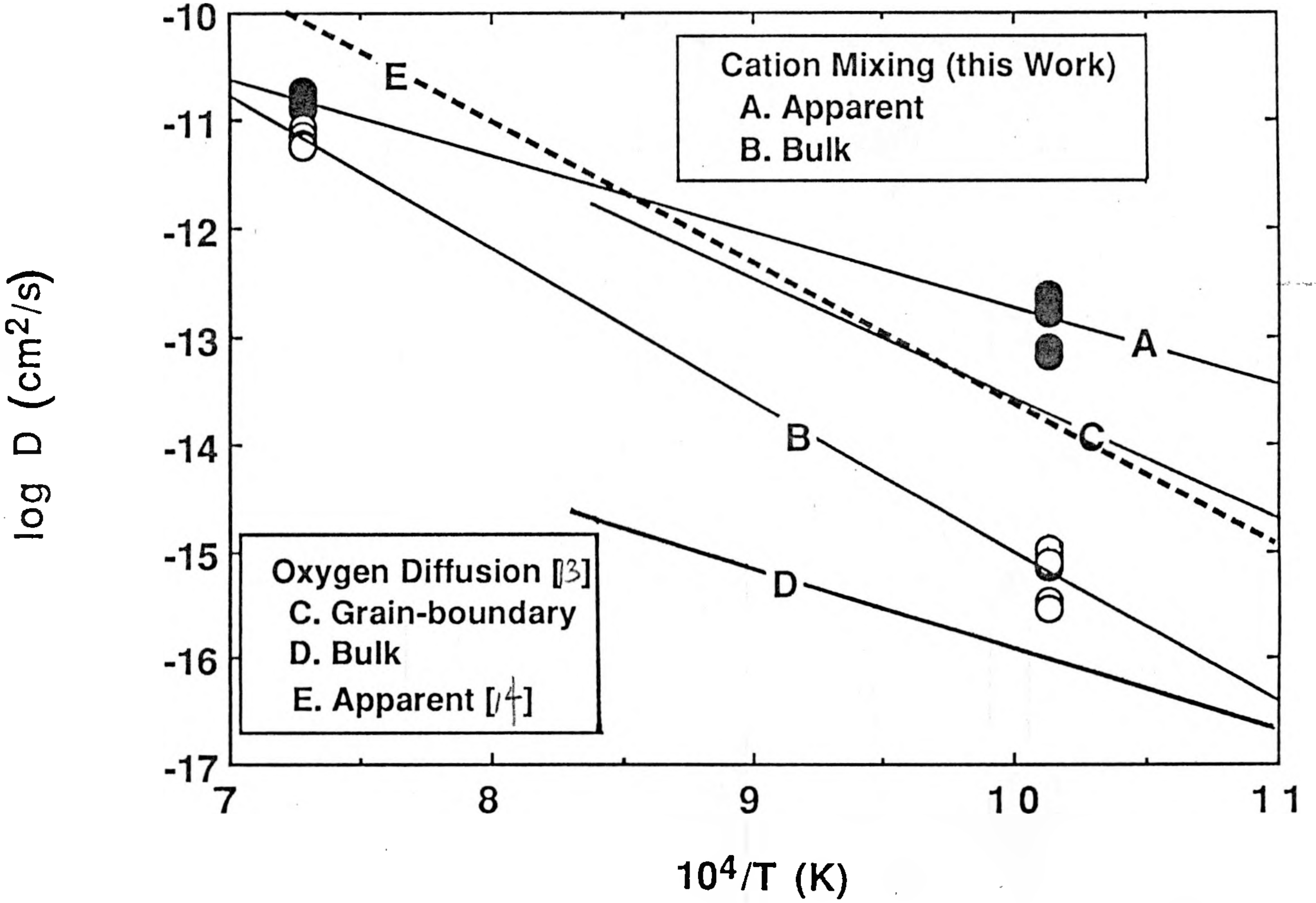
Cation Mixing (this Work)
A. Apparent
B. Bulk
Oxygen Diffusion [13]
C. Grain-boundary
D. Bulk
E. Apparent [14]
A
B
C
D
E
log D (cm^2/s)
-10
-11
-12
-13
-14
-15
-16
-17
7
8
9
10
11
10^4/T (K)

ⓑ